sciendo

Prompt gamma-ray methods for industrial process evaluation: A simulation study

Mohammed Siddig H. Mohammed [ID],
Abdulsalam Alhawsawi [ID],
M. S. Aljohani,
Mohammed M. Damoom,
Essam M. Banoqitah [ID],
Ezzat Elmoujarkach [ID]

Abstract. Radioisotope applications in industrial process inspection and evaluation using gamma-ray emitters provide otherwise unavailable information. Offering alternative gamma-ray sources can support the technology by complementing sources' availability and radiation safety. This work proposes to replace gamma-ray from radioisotopes with prompt gamma-ray from the interaction of neutrons with stable isotopes injected into the industrial process or with the structural material of the industrial process equipment. Monte Carlo N-Particle Transport Code (MCNP5) was used to simulate the irradiation of two-phase flow pipes by ^{252}Cf neutron source. Two simulations were run for each pipe, with and without mixing the liquid phase with the stable isotope ^{157}Gd. The detected gamma-ray spectra were analysed, and images of the two phases inside the pipes were produced. The images were compared to images obtained from simulations of gamma transmission measurement using ^{60}Co. Furthermore, results for prompt gamma computed tomography (CT) were presented and discussed. The studies' outcomes indicate the potential of prompt gamma-ray to carry out the sealed sources applications of gamma transmission measurements and imaging.

Keywords: Prompt gamma-ray • Sealed sources • Radiotracers • Industrial process

M. S. H. Mohammed✉, A. Alhawsawi, M. S. Aljohani,
M. M. Damoom, E. M. Banoqitah, E. Elmoujarkach
King Abdulaziz University
Department of Nuclear Engineering
P. O. Box 80204, Jeddah, 21589, Saudi Arabia
E-mail: msmohamad@kau.edu.sa

Introduction

Radiotracers and sealed radioactive sources are used to obtain information about the process equipment's operation. The information is used for equipment diagnosis, optimization of the processes, and modelling of multiphase flows.

In radiotracer applications, radioactive material in physical and chemical compatibilities with the process material is injected into the process equipment and monitored with radiation detectors between the inlet and outlet to reveal the behaviour of the traced material. Examples of radiotracers used in industry are technetium-99m (^{99m}Tc) and tritium (^{3}H) for the aqueous phase, bromine-82 (^{82}Br) and iodine-131(^{131}I) for organic phase, gold-198 (^{198}Au) and lanthanum-140 (^{140}La) for solid phase, and argon-41 (^{41}Ar) for gases. Radiotracer techniques have been used to understand the process and bring about improvement in the chemical industry [1], to determine the mixing efficiency in industrial applications [2], to make use of residence time distribution (RTD) measurements to analyse complex flow [3], and to detect lining wear, and location of pipelines leaks [4]. The advancements in the methodology include radioactive particle tracking (RPT), which has been used to investigate the hydrodynamic parameters in bubble column reactor [5], study solids motion in a fluidized bed [6], and fluid tracking [7].

Imaging using the single photon emission computed tomography (SPECT) is another advanced radiotracer modality [8, 9].

The other group of radioisotope techniques uses sealed radioactive sources. Gamma-ray sources like cobalt-60 (^{60}Co) and cesium-137 (^{137}Cs) are placed on one side of the process equipment and a radiation detector on the opposite side to measure the transmitted radiation, which is then correlated to the densities of the process materials. Gamma scanning and tomography have been used for the inspection of distillation columns [10, 11], and used for the detection of pipelines anomalies [12–14].

The substantial technological solutions and economic benefits of radioisotope applications come with the drawbacks of gamma-ray emitters availability, risk of contamination, and radioactive waste. The nuclear reactors that produce the radioisotopes are not available in all countries, and so there is a need to import them from other countries, which is time-consuming and does not fit the requirements of the urgent jobs, especially for short-lived radioisotopes. Radiotracers are open radioactive sources, and therefore, there is always a risk of contamination during shipping, preparation, and injection into the process equipment. After applying the radiotracers, radioactive material in the process stream or drain should be treated as radioactive waste. The level of the radioactivity in the waste depends on the concentration, half-life, radioactivity, and energy of the radioisotope. The gamma-ray sealed sources are associated with lesser or moderate concerns than radiotracers; nevertheless, offering alternatives will support technology convenience and enhance radiation safety.

This work investigates the use of neutron sources to irradiate the structural material of the process equipment and stable isotopes injected into the process to prompt gamma-ray as an alternative to gamma-ray emitters applied to the industrial process investigations. Neutrons are used in industrial diagnosis under the category of sealed sources applications in level measurement in storage tanks and chemical reactors [15, 16]. Other neutrons' industrial applications include neutron radiography [17–19], neutron CT [20], and in moisture-based measurements like in paper industry [21]. In medical imaging, neutron activation and prompt gamma have been used for SPECT imaging and during boron neutron capture therapy (BNCT) [22, 23]. Neutrons have not been used to produce gamma-ray for the radiation technology used in industrial process units.

The investigations in this paper aim to propose novel methods that use prompt gamma-ray for industrial process evaluation. The methods could provide options that overcome some of the limitations of gamma-ray sources and supplement industrial neutron applications.

Method

The research's first hypothesis was to replace the gamma-ray emitters in industrial process gamma
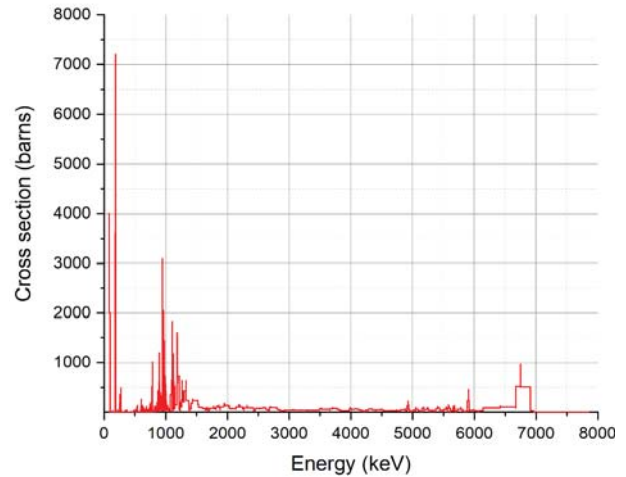

Fig. 1. Prompt gamma-ray spectrum of the reaction ^{157}Gd (n, γ).

emission tomography and other radiotracer applications with the stable isotope gadolinium-157 (^{157}Gd), which emits prompt gamma-ray after neutron irradiation. The ^{157}Gd was chosen because of its large capture cross-section for thermal neutrons to act as a tracer of the liquid phase (water) in a pipe. The neutrons emitted from a source in contact with the pipe's exterior surface will be thermalized after passing through the liquid phase inside the pipe. Then, the thermal neutron reaction ^{157}Gd $(n, \gamma)^{158}$Gd releases gamma ray due to the de-excitation of ^{158}Gd (Fig. 1).

The fast neutron interaction with the pipe's wall material and water molecules will also emit prompt gamma that will be characterized, and its contribution to the radiation reaching the detector will be analysed.

The neutron source used in this paper's studies was a californium-252 (^{252}Cf) spontaneous fission neutron source, with the spectrum depicted in Fig. 2. The gamma-ray associated with the fission of ^{252}Cf has not been accounted for in the simulation studies.

The simulations were run using the Monte Carlo N-Particle Transport Code (MCNP5) [24]. The setup shown in Fig. 3 consists of a carbon steel pipe, a liquid phase (water) that occupies half of the pipe's
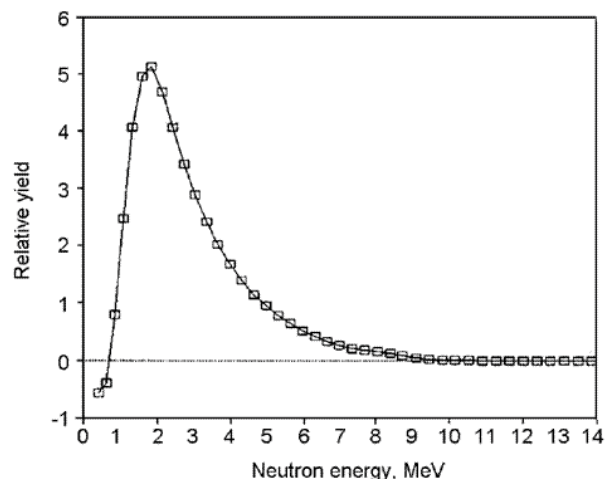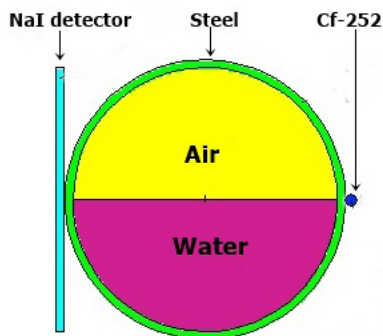

Fig. 2. Neutron spectrum of ^{252}Cf.

Fig. 3. Simulation setup.

volume, a gaseous phase (air) that occupies the other half, ^{252}Cf source placed on the exterior surface of the pipe at the position of the interface of the two phases, and a NaI detector in the opposite side to the neutron source. The detector was modelled with dimensions of 30 cm × 30 cm × 3 cm and a resolution of 124 × 124 pixels.

The water was dopped with a ^{157}Gd concentration equivalent to 5% of the water volume, which was decided after investigating the effect of different ^{157}Gd concentrations on the emitted prompt gamma's intensity.

The second hypothesis was that the fast neutron interaction with the pipe's wall material will induce prompt gamma-ray due to the inelastic scattering interaction ^{56}Fe (n, n', γ) ^{56}Fe. The prompt radiation could be used for gamma transmission measurements. The hypothesis was tested using the same simulation setup described above, except that there was no added ^{57}Gd.

The results of the hypothesis testing were compared to results of simulations using cobalt-60 (^{60}Co) having a radioactivity of 10 mCi.

The investigative experiments of both hypotheses were simulated using three pipes having diameters of 10 cm, 20 cm, and 30 cm, and the wall thicknesses were 2 mm, 6 mm and 9 mm, respectively.

Results and discussion

Simulations were run to determine the yield of the neutron source that is required to produce adequate image quality. The simulations used ^{252}Cf and the 10 cm diameter-pipe with different yields ranging from 1×10^5 neutron/second to 5×10^8 neutron/s with 1×10^5 interval (i.e., 1×10^5, 2×10^5, 3×10^5, ..., 5×10^8). The ^{252}Cf yield of 2×10^7 neutron/s, obtained from a source with a 4.6 mCi activity, was deemed the minimum to achieve the imaging task. Further increasing the source strength enhanced the image quality; however, no significant improvement was observed beyond 1×10^8 neutron/s.

Using 1×10^8 neutron/s for imaging the other two pipes (having 20 cm and 30 cm diameters) produced satisfactory image quality, and therefore, this yield was used in the simulation setup.

Concerning the first hypothesis, the prompt gamma spectra obtained from the simulation of
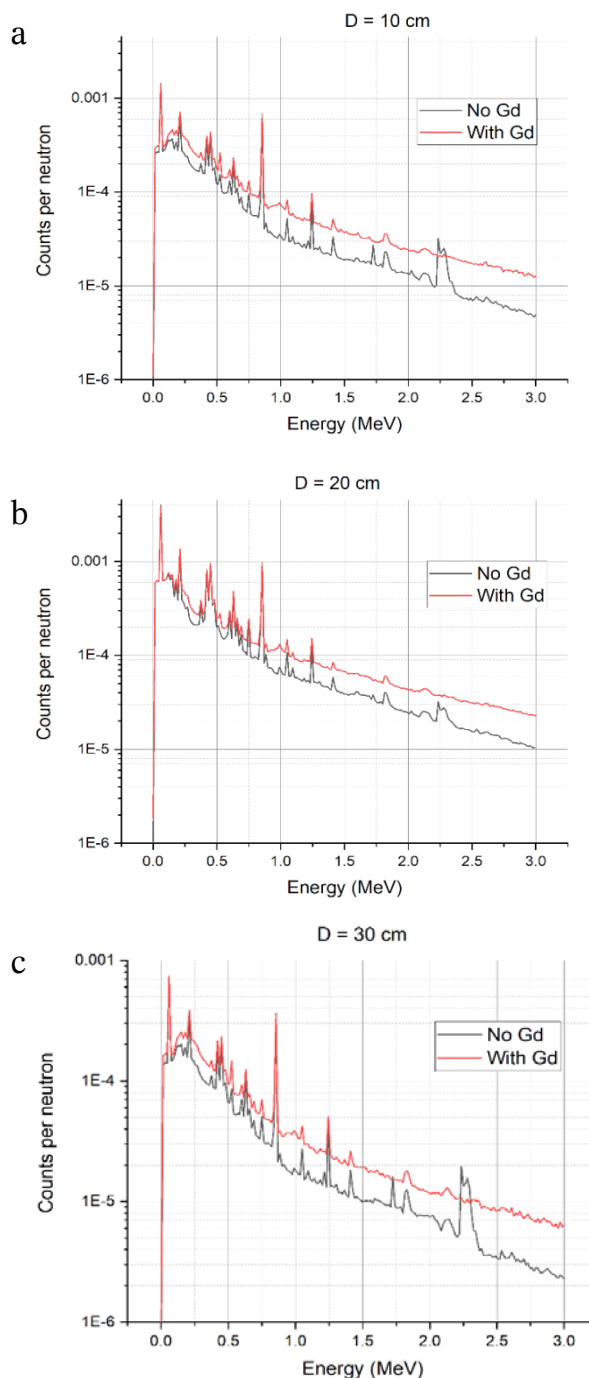

Fig. 4. The gamma-ray spectrum obtained in the simulation: the pipe with a diameter of 10 cm (a), 20 cm (b), and 30 cm (c).

the three pipes irradiation by neutrons are shown in Figs. 4a–c. Each pipe irradiation was simulated in two runs before and after mixing the water with ^{157}Gd. The effect of the ^{157}Gd caused the addition of energy peaks and an increase in the energies' overall intensity. The prompt gamma-ray spectrum showed numerous ^{157}Gd gamma energies lines, but the significant energies are 182 KeV and 944 KeV.

The data in Table 1 details the interactions (per neutron) with the involved materials in the simulation of the 10 cm-pipe irradiation. The significant photon production was from ^{157}Gd, ^{56}Fe, and the detector crystal.

Table 1. Neutrons interactions with air, water, gadolinium, steel, and the detector

Material	Nuclides	Atom fraction	Total collisions	Collisions weight	Weight lost to capture	Photons produced	Photon weight produced%
Air	C	1.50E–04	4	1.68E–08	0.00E+00	0	0.00
	N	7.84E–01	49 813	2.09E–04	1.06E–05	515	2.16E–04
	O	2.11E–01	15 614	6.55E–05	2.77E–07	42	1.76E–05
	Ar	4.67E–03	309	1.30E–06	0.00E+00	66	2.77E–05
Water + 5% Gd	H	6.65E–01	193 776 900	8.13E–01	2.67E–04	35 038	1.47E–02
	O	3.33E–01	37 866 142	1.59E–01	4.52E–04	91 459	3.84E–02
	^{157}Gd	2.01E–03	6 394 471	2.68E–02	2.37E–02	19 207 904	8.25E–02
Steel	C	2.28E–02	484 984	2.03E–03	1.46E–06	2 726	1.14E–03
	Fe	9.77E–01	29 489 449	1.24E–01	5.04E–04	7 955 587	3.34E–02
NaI	Na	5.00E–01	8 353 033	3.50E–02	4.11E–05	1 276 750	5.36E–03
	I	5.00E–01	14 164 504	5.94E–02	1.88E–03	8 494 594	3.56E–02

Radiation dose calculations at different distances were carried out to investigate the radiation protection measures required to account for the quantity of the transmitted and scattered neutrons from the 10 cm pipe. Figures 5 and 6 depict the neutron source in the center of circles and the neutron dose rates at different radii measured every 45°, with 0° being in the straight line in front of the neutron source and the sample. The calculations were performed for distances from 1 m to 15 m; however, the figures present selected four radii for each case.

Figure 5 shows the dose rates from a source with the 2×10^7 neutron/s yield (the minimum to achieve reasonable image quality), and Fig. 6 shows the dose rates from a source with an output of 1×10^8 neutron/s. In both cases, the dose rates were much higher at the back and sides of the source because the source is unshielded nor collimated.

If 7.5 μSv/h is considered the maximum permitted dose rate that defines the controlled area at the worksite, 6 m was enough distance to demarcate the area when the minimum activity was used. The radius of the area when the maximum activity was used was 13 m.

The dose rates at the controlled and supervised areas can be further decreased when using shielding and collimation.

Changing the pipe diameter from 10 cm to 20 cm resulted in a higher intensity due to the increased water path that enabled better thermalization and a larger interaction volume, which yielded a higher amount of prompt gamma. However, changing the diameter to 30 cm caused the overall intensity to decrease, attributed to distance attenuation.

Images were produced for the visualization of the pipe's flow. For the pipe with a diameter of 10 cm
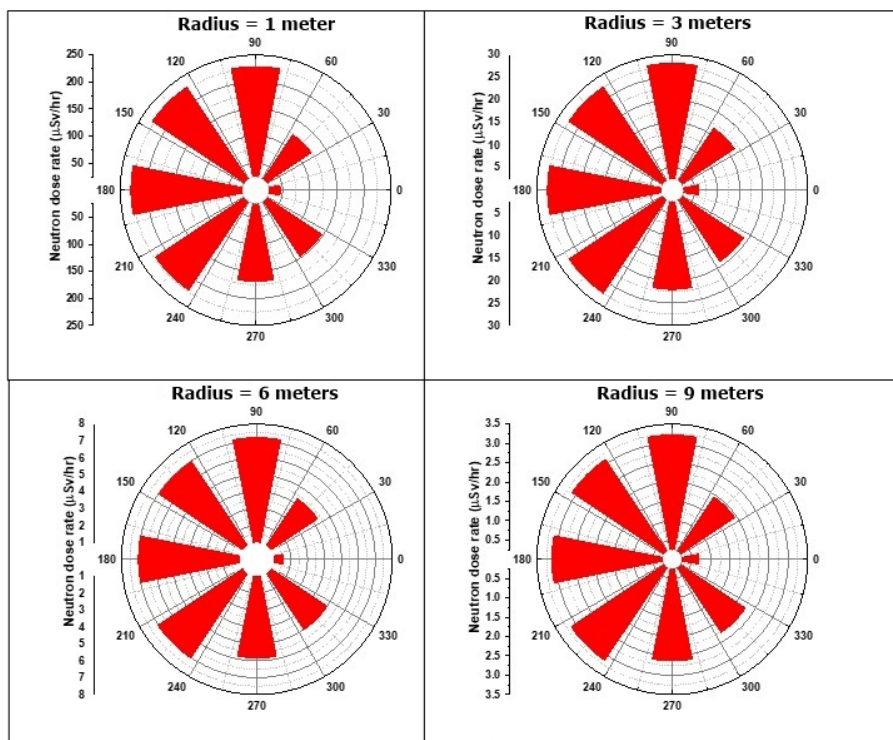
Fig. 5. Neutron dose rates from the neutron source with the minimum activity at different radii.
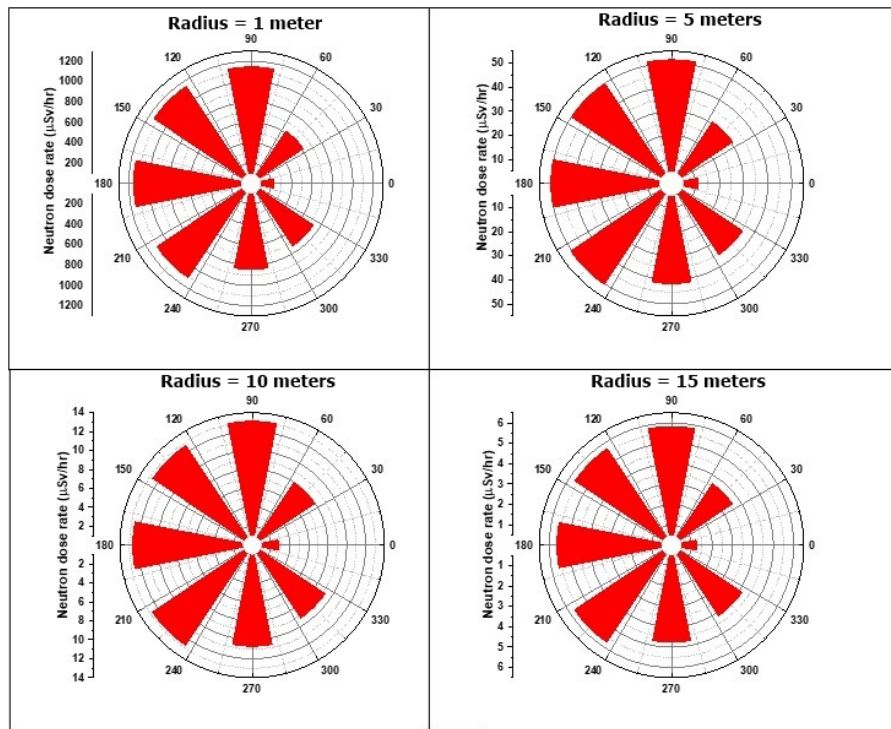
Fig. 6. Neutron dose rates from the neutron source with the maximum activity at different radii.

irradiated by the neutron source before adding ^{157}Gd (Fig. 7a), the gamma-ray intensity measured from the air-side (yellow and orange colours) was much higher than that received from the water-side, with the blue colour (Fig. 7b). The higher intensities were due to the less attenuated gamma-ray resulting from neutrons' interaction with ^{56}Fe and the gas mixture of the air.

The addition of ^{157}Gd caused the intensity of the radiation from the water-side to increase, but it was still lower than that from the air-side. Therefore, although the contrast between the two phases was evident in the two cases, it was better distinct in the images obtained without ^{157}Gd.

The same analysis applies to the 20 cm and 30 cm diameter pipes; nevertheless, the intensities from the ^{157}Gd in the water-side decrease with the increasing distance due to attenuation caused by the increased distance and water path. Figures 7a–f show the simulation results of the three pipes.

The difference between the radiation intensities transmitted by the two phases counters the research's first assumption that the prompt gamma
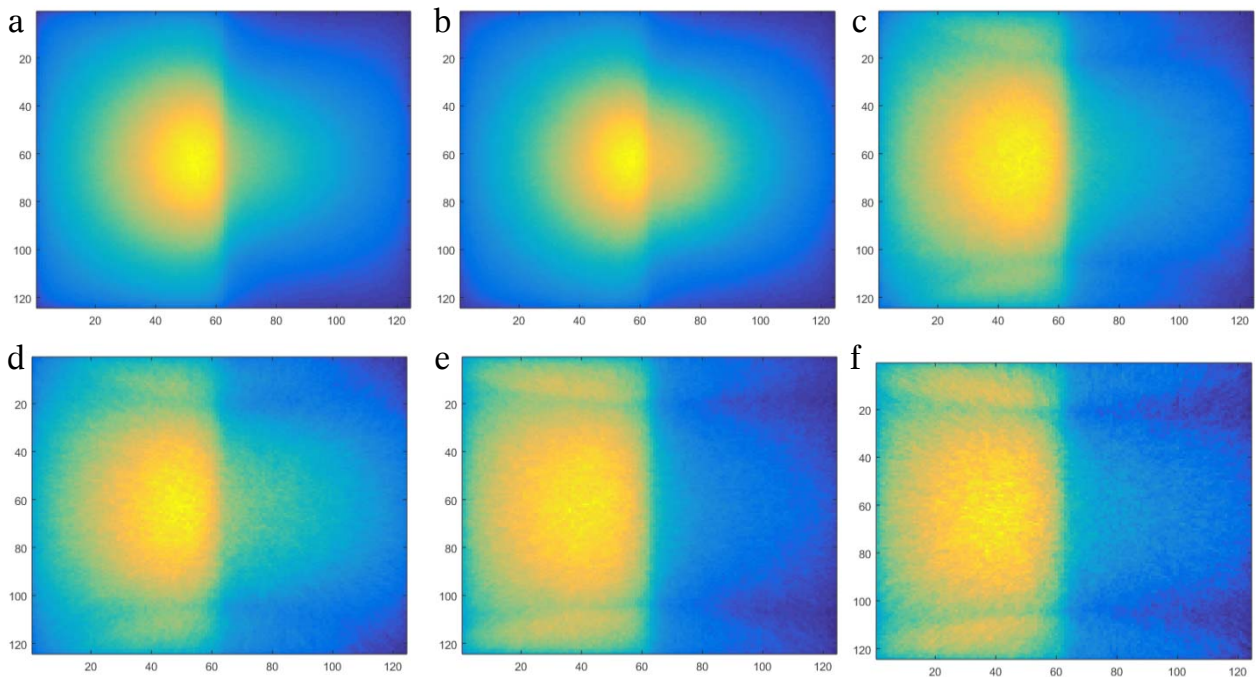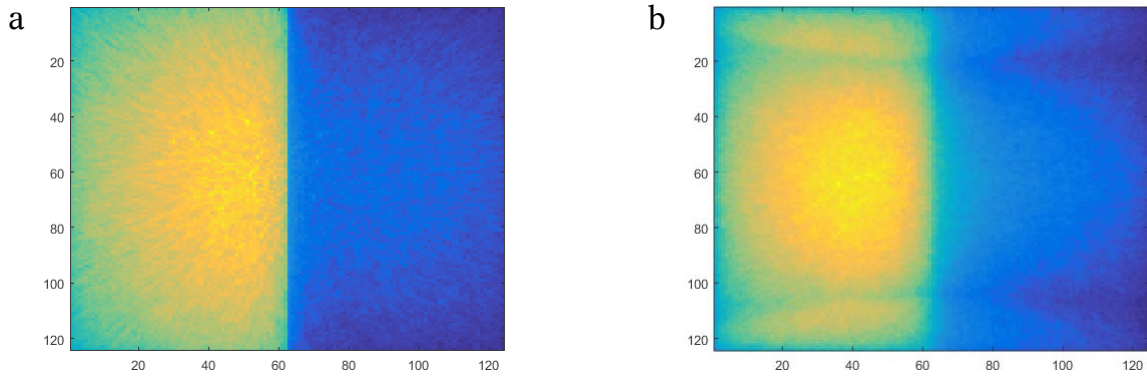

Fig. 7. The pipe with a diameter 10 cm without ^{57}Gd (a) and with ^{57}Gd (b). The pipe with a diameter 20 cm without ^{57}Gd (c) and with ^{57}Gd (d). The pipe with a diameter 30 cm without ^{57}Gd (e) and with ^{57}Gd.

Fig. 8. Imaging of the pipe with diameter 30 cm using ^{60}Co (a) and prompt gamma-ray (b). (Fig. 8b is reproduced from Fig. 7e).

from the liquid phase will be higher. The radiation from the liquid phase may be increased by increasing the concentration of ^{157}Gd. Still, it would be an impractical option because it requires a large amount of ^{157}Gd to the pipe's volume, and it is not certain to affect a significant intensity increase.

The results do not favour the first hypothesis, as the gamma-ray intensity of the proposed ^{157}Gd tracer is insufficient to characterize the liquid phase. However, identification of some disruptions like bubbles or solid deposits in small diameter pipes using the detected radiation can be further investigated.

The previously described results were compared to a simulation of imaging the 30 cm diameter pipe using ^{60}Co (Fig. 8) to test the second research hypothesis concerning gamma-ray transmission measurements, which uses radiation sealed sources. The definition of the images produced using ^{60}Co was slightly better than that obtained when the neutrons were used to prompt gamma-ray from the pipe's wall material without mixing the water with ^{57}Gd. The imaging used the total gamma ray prompted due to the interaction with steel, air, water, and detector crystal. For accurate gamma transmission imaging, further study is needed to quantify the various radiation intensity components reaching the detector and explore filtering methods.

The prompt gamma-ray method could be an advantageous alternative if a D-D neutron generator, which has an energy comparable to that of ^{252}Cf, is used. Using a neutron generator overcomes the challenge of ^{252}Cf availability. Furthermore, it could provide a reasonable trade-off between image quality and radiation safety, considering the exposure time and ability to control radiation exposure.

A published application note recommended using a hybrid system that combines gamma transmission and neutron backscatter principles to maximize the benefits in monitoring coke drums [25]. The system consists of a neutron gauge and gamma measurement device that uses ^{137}Cs. Another study proposed the deployment of both neutrons and gamma-ray of ^{252}Cf by simultaneously measuring the backscatter of the two types of radiation to detect corrosion defects in pipelines [26].

The study presented in this work about using neutrons to prompt gamma from the material of the process equipment unfolds the possibility to apply the principles of gamma-ray transmission and neutron backscattering simultaneously using one device and offering better cost and radiation safety effectiveness. Incorporating gamma backscatter measurement in the system adds a dimension that can make an integrated nuclear device for process monitoring.

To examine prompt gamma transmission for different neutron source positions and explore the feasibility of gamma transmission tomography, a simulation of CT was run. The CT was implemented by moving the source and the detector simultaneously around the pipe circumference and taking measurements every 72°. The obtained projections were processed in MATLAB using the Ordered Subset Expectation Maximization (OSEM) reconstructions algorithm. The reconstructed images are shown in Fig. 9, indicating the prompt gamma's success in performing CT. The much lower radiation intensity in the water-side indicated by the light blue colour is due to interaction of neutrons with hydrogen and oxygen. The interface between the two phases was not sharply defined like it was in the single projections in Fig. 8, which can
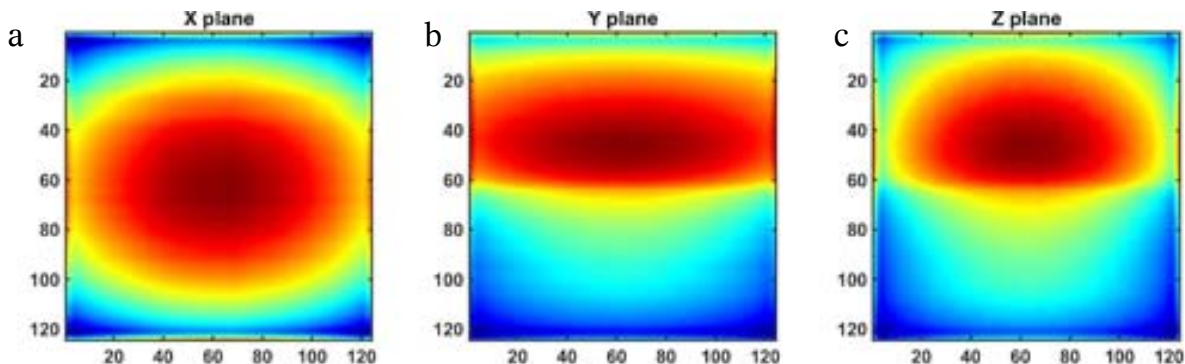
Fig. 9. Reconstructed prompt gamma CT images: (a) X plane, (b) Y plane, (c) Z plane.

be attributed to higher radiation from the water as a result of the summation of five detectors measurements, number, and positions of the detectors, or a possible shortcoming of the reconstruction algorithm.

Utilizing prompt gamma-ray from ^{157}Gd to identify bubbles or solid deposits in small diameter pipes and applying neutron generators to replace radiation sealed sources for gamma transmission measurements and tomography need further itemized simulation studies to analyse the feasibility and the required experimental validation.
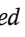
Conclusion

The simulation studies showed that the prompt gamma-ray intensity due to neutrons' interaction with ^{157}Gd and water is less than that of the interaction with the pipe wall material and the air. Therefore, the results indicate the difficulty of replacing the radiotracers with ^{157}Gd; however, the results also suggest neutron sources' potential and prompt gamma as an alternative to gamma-ray sources in the sealed sources applications in industrial plants.

Moreover, the use of neutrons enables to combine the applications of neutron backscattering, gamma-ray backscattering, and gamma-ray transmission measurement or tomographic imaging in a single system with the prompt gamma-ray method, offering a cost-effective option and moderating the radiation safety burden or even almost eliminating it if a neutron generator is used instead of an isotopic source. The future work considers a comprehensive experimental validation, including the requirements of the detection system to characterize the transmitted gamma-ray based on its origin, whether it is prompt radiation due to the interaction with the present materials or gamma-ray emissions of the ^{252}Cf, and the required filtering methods.

ORCID

A. M. Alhawsawi http://orcid.org/0000-0002-7992-8850
E. M. Banoqitah http://orcid.org/0000-0002-9127-6322
E. Elmoujarkach http://orcid.org/0000-0003-2750-5984
M. S. H. Mohammed http://orcid.org/0000-0002-4238-9566

References

1. Mohd Yunos, M. A. S., Hussain, S. A., Mohamed Yusoff, H., & Abddullah, J. (2016). Industrial radiotracer technology for process optimizations in chemical industries – A review. *Pertamika J. Scholarly Res. Rev.*, 2(3), 20–46. https://core.ac.uk/download/pdf/234560224.pdf.

2. Othman, N., & Kamarudin, S. K. (2014). Radiotracer technology in mixing processes for industrial applications. *Sci. World J.*, *2014*, 1–15. DOI: 10.1155/2014/768604.

3. Thyn, J., & Zitny, R. (2004). Radiotracer applications for the analysis of complex flow structure in industrial apparatuses. *Nucl. Instrum. Methods Phys. Res. Sect. B-Beam Interact. Mater. Atoms*, *213*, 339–347. DOI: 10.1016/S0168-583X(03)01648-3.

4. Eapenm, A. C., Raom, S. M., Agashem, S. M., Ajmera, R. L., & Yelgaonkar, V. N. (1990). Radiotracer applications in steel, petroleum and maritime industries with significant economic benefits. *Isot. Environ. Health Stud.*, *26*(9), 424–429. DOI: 10.1080/10256019008624349.

5. Mohd Yunos, M. A. S., Sipaun, S. M., & Hussain, S. A. (2019). Feasibility of using radioactive particle tracking as an alternative technique for experimental investigation in bubble column reactor. *IOP Conf. Ser. Mater. Sci. Eng.*, *554*, 012005. DOI: 10.1088/1757-899X/554/1/012005.

6. Lin, J. S., Chen, M. M., & Chao, B. T. (1985). A novel radioactive particle tracking facility for measurement of solids motion in gas fluidized beds. *AIChE J.*, *31*(3), 465–473. DOI: 10.1002/aic.690310314.

7. Vieira, W. S., Brandão, L. E. B., & Braz, D. (2014). An alternative method for tracking a radioactive particle inside a fluid. *Appl. Radiat. Isot.*, *85*, 139–146. DOI: 10.1016/j.apradiso.2013.12.006.

8. International Atomic Energy Agency. (2008). *Industrial process gamma tomography*. Vienna: IAEA. (IAEA-TECDOC-1589). Available from https://www-pub.iaea.org/MTCD/Publications/PDF/TE_1589_web.pdf.

9. Wang, M. (2015). *Industrial tomography*. Elsevier. https://doi.org/10.1016/C2013-0-16466-5.

10. Abdullah, J. (2005). Gamma-ray scanning for troubleshooting, optimisation and predictive maintenance of distillation columns. *Hydrocarbon Asia*, 1/2, 62–65. https://scanningtech.com/PDF/article3.pdf.

11. Haraguchi, M. I., Kim, H. Y., Sprenger, F. E., & Calvo, W. A. P. (2012). Industrial equipment troubleshooting with imaging technique improved gamma-ray absorption scans. *J. Phys. Sci. Appl.*, *2*(8), 359–371.

12. Suma, T., Yelgaonkar, V. N., Tiwari, C. B., & Dhakar, V. D. (2016). Detection of interfaces and voids in pipelines using gamma scanning. *IOSR J. Appl. Phys.*, *8*(04), 12–26. DOI: 10.9790/4861-0804011226.

13. Askari, M., Taheri, A., Mojtahedzadeh Larijani, M., Movafeghi, A., & Faripour, H. (2019). A gamma-ray tomography system to determine wax deposition distribution in oil pipelines. *Rev. Sci. Instrum.*, *90*(7), 075103. DOI: 10.1063/1.5095859.

14. Saengchantr, D., Srisatit, S., & Chankow, N. (2019). Development of gamma ray scanning coupled with computed tomographic technique to inspect a broken pipe structure inside laboratory scale vessel. *Nucl. Eng. Technol.*, *51*(3), 800–806. DOI: 10.1016/j.net.2018.12.022.

15. Zain, R. M., Yahya, R., Rahman, M. F., & Yusof, N. M. (2015). Neutron imaging system for level interface measurement. In Malaysia International NDT Conference & Exhibition 2015 (MINDTCE-15), November 2015, pp. 22–24. https://www.ndt.net/events/MINDTCE-15/app/content/Paper/26_Zain.pdf.

16. Zain, R. M., Ithnin, H., Razali, A. M., Yusof, N. H. M., Mustapha, I., Yahya, R., Othman, N., & Rahman, M. F. A. (2017). Slow neutron mapping technique for level interface measurement. *AIP Conf. Proc.*, *1799*, 050004. DOI: 10.1063/1.4972938.

17. Bishnoi, S., Sarkar, P., Thomas, R., Patel, T., & Gadkari, S. (2016). Fast neutron radiography with DT neutron generator. *Non-Destruct. Eval.*, *22*, 68–73.

18. Bishnoi, S., Thomas, R. G., Sarkar, P. S., Datar, V. M., & Sinha, A. (2015). Simulation study of fast neutron radiography using GEANT4. *J. Instrum.*, *10*(02), P02002–P02002. DOI: 10.1088/1748-0221/10/02/P02002.

19. International Atomic Energy Agency. (2008). *Neutron imaging: A non-destructive tool for materials testing.* Vienna: IAEA. Available from https://www-pub.iaea.org/MTCD/Publications/PDF/te_1604_web.pdf.

20. Schillinger, B. (2019). An affordable image detector and a low-cost evaluation system for computed tomography using neutrons, X-rays or visible light. *Quantum Beam Sci.*, *3*(4), 21. DOI: 10.3390/qubs3040021.

21. Hasan, N. M., Zain, R. M., Abdul Rahman, M. F., & Mustapha, I. (2009). The use of a neutron backscatter technique for in-situ water measurement in paper-recycling industry. *Appl. Radiat. Isot.*, *67*(7/8), 1239–1243. DOI: 10.1016/j.apradiso.2009.02.020.

22. Bell, A. R., McRae, G., Wassenaar, R., & Wells, G. (2011). Neutron activation for planar and SPECT imaging. In IEEE International Symposium on Biomedical Imaging: From Nano to Macro, March 2011, pp. 1801–1804. DOI: 10.1109/ISBI.2011.5872756.

23. Kim, M. -S., Shin, H. -B., Choi, M. -G., Monzen, H., Shin, J. G., Suh, T. S., & Yoon, D. -K. (2020). Reference based simulation study of detector comparison for BNCT-SPECT imaging. *Nucl. Eng. Technol.*, *52*(1), 155–163. DOI: 10.1016/j.net.2019.07.002.

24. X-5 Monte Carlo Team. (2008). *MCNP – A General Monte Carlo N-Particle Transport Code, Version 5. Volume I: Overview and theory.* Los Alamos National Security, LLC. Available from https://laws.lanl.gov/vhosts/mcnp.lanl.gov/pdf_files/la-ur-03-1987.pdf.

25. Hart, T. (2015). *Neutron backscatter versus gamma transmission analysis for coke drum applications.* Thermo Scientific. Available from http://tools.thermofisher.com/content/sfs/brochures/EPM-ANCoker-0215.pdf.

26. Licata, M., Aspinall, M. D., Bandala, M., Cave, F. D., Conway, S., Gerta, D., Parker, H. M. O., Roberts, N. J., Taylor, G. C., & Joyce, M. J. (2020). Depicting corrosion-born defects in pipelines with combined neutron/γ ray backscatter: a biomimetic approach. *Sci. Rep.*, *10*(1), 1486. DOI: 10.1038/s41598-020-58122-3.